RSC Advances

ROYAL SOCIETY OF CHEMISTRY

www.rsc.org/advances

Cite this: DOI: 10.1039/c0xx00000x

www.rsc.org/xxxxxx

ARTICLE TYPE

Synthesis, characterization and properties of Ce-modified $S_2O_8^{2-}/ZnAl_2O_4$ solid acid catalysts

Jun-Xia Wang,*[a] An-Qi Wang,[a] Yu-Lin Xing,[a] Zheng-Xin Zhu,[a] Xiu-Ling Wu,[a] Yong-Qian Wang[a] and Li-Xia Yang[a]

Received (in XXX, XXX) Xth XXXXXXXXX 20XX, Accepted Xth XXXXXXXXX 20XX
DOI: 10.1039/b000000x

Abstract: A new spinel solid acid catalyst of $S_2O_8^{2-}/ZnAl_2O_4$-*x* wt%Ce was simply prepared by modifying $S_2O_8^{2-}/ZnAl_2O_4$ with Ce for acid catalysis of acetic acid and *n*-butanol. The prepared catalysts were characterized by means of XRD, IR, TG, XPS, NH_3-TPD, SEM and N_2-physisorption. The experimental results showed $S_2O_8^{2-}/ZnAl_2O_4$-*x* wt%Ce solid acid catalysts belonged to spinel-type $ZnAl_2O_4$ structure. The addition of Ce played a key role in stabilizing the surface sulfur species and consequently increasing the acid strength of $S_2O_8^{2-}/ZnAl_2O_4$-*x* wt%Ce. The appropriate modification of Ce was 4 wt% and $S_2O_8^{2-}/ZnAl_2O_4$-4 wt%Ce catalyst had 95.9% esterification efficiency under the optimum reaction conditions. Compared with unmodified $S_2O_8^{2-}/ZnAl_2O_4$ catalyst, $S_2O_8^{2-}/ZnAl_2O_4$-4 wt%Ce solid acid catalyst showed much better reusability, which could remain above 80% esterification even after being used for six times. The loss of sulfur species on the surface of $S_2O_8^{2-}/ZnAl_2O_4$-4 wt%Ce solid acid was one of the essential reasons for its deactivation during the acid catalyzed reaction.

1. Introduction

In recent years, acid catalysts have been widely used in many acid catalytic reactions, including dehydration, isomerization, acylation, esterification, alkylation and polymerization, etc. Conventional industrial acid catalysts, such as inorganic acids (e. g. H_3PO_4, HCl, H_2SO_4, etc.) and Lewis acids (e. g. $AlCl_3$, $TiCl_4$, etc.), have unavoidable drawbacks because of their severe corrosivity and environmental problems. To overcome these disadvantages, a number of heterogeneous solid acid catalysts, such as ion exchange resin, sulfonated-carbon materials, zeolites, heteropoly acids, niobium oxide, sulphated metal oxides (SO_4^{2-}/M_xO_y), etc, have been studied because of their significant advantages of easy recovery, few disposals, less corrosion, and environmental safety. [1-5] Nowadays, solid acid catalysts has been tested for many organic reactions, such as esterification, sugar dehydration, *n*-alkanes isomerization, condensation reaction, acetalization reaction, and so forth. [6-9] The SO_4^{2-}/M_xO_y is an interesting class of solid acid catalysts because of its unique advantages. [10, 11] For example, it has been demonstrated that it is easy to synthesize and presents other advantages of better thermal stability, stronger acidity and higher catalytic activity in many kinds of organic reactions even at very mild conditions. However, SO_4^{2-}/M_xO_y solid acid catalysts, including two representative systems of SO_4^{2-}/ZrO_2 and SO_4^{2-}/TiO_2, usually surfer from low stability and rapid deactivation, which limit their promising practical applications. [12, 13] To overcome these drawbacks, numerous approaches have been employed over the past several decades. Among them, the modification of SO_4^{2-}/M_xO_y with other metallic ions is typically considered as an effective method to greatly improve the acid sites dispersion, stabilize the surface sulfur species and enhance the stability of SO_4^{2-}/M_xO_y solid acid catalysts. [14-18] However, crystal structure transformation will inevitably happen in the process of modification SO_4^{2-}/M_xO_y solid acid with other metallic ions. Moreover, this phenomenon is difficult to control and leads to a negative effect on the catalytic performances of SO_4^{2-}/M_xO_y solid acid catalysts. [19-21] So, the quest for new superior systems that avoids the above disadvantages of SO_4^{2-}/M_xO_y has led to exploration of alternative metal oxides as a substitute for synthesis of SO_4^{2-}/M_xO_y solid acid catalysts. In our preliminary experiment, we had identified that composite oxide spinel $ZnAl_2O_4$ could be successfully used in synthesis of $S_2O_8^{2-}/ZnAl_2O_4$ spinel solid acid, which had exhibited high catalytic activity in the esterification of *n*-butyl acetate. Particularly, $S_2O_8^{2-}/ZnAl_2O_4$ had the prominent advantages of stable structure owing to its single spinel crystal shape. [22] However, for unmodified $S_2O_8^{2-}/ZnAl_2O_4$ solid acid catalyst, there were still similar disadvantage of the relatively short lifetime and low reusability with other SO_4^{2-}/M_xO_y solid acid catalysts. Therefore, directions for further improving its catalytic properties include modifying $S_2O_8^{2-}/ZnAl_2O_4$ with other promoters.

Based on the above background, the present work makes an attempt on modifying $S_2O_8^{2-}/ZnAl_2O_4$ with Ce. The main aim of this paper is to investigate the effect of Ce modification on acidic properties, the catalytic activities and the stability of $S_2O_8^{2-}/ZnAl_2O_4$ spinel solid acid in detail. For this purpose, a new spinel solid acid catalyst of $S_2O_8^{2-}/ZnAl_2O_4$-*x* wt%Ce was simply

prepared by modifying $S_2O_8^{2-}/ZnAl_2O_4$ with Ce for acid catalysis of acetic acid and *n*-butanol in this paper. In addition, synthesis conditions of $S_2O_8^{2-}/ZnAl_2O_4$-4wt%Ce solid acid catalyst were optimized, including reaction times, acetic acid/*n*-butanol ratio and catalyst amounts. In the meantime, the reusability of $S_2O_8^{2-}/ZnAl_2O_4$-4wt%Ce solid acid catalyst was also evaluated. The catalyst structure and the acidic activity of $S_2O_8^{2-}/ZnAl_2O_4$-*x* wt%Ce solid acid catalysts were characterized by XRD, IR, TG, NH_3-TPD, XPS, SEM and N_2-physisorption techniques. Up to now, there are few reports about the reasons for deactivation of SO_4^{2-}/M_xO_y solid acid catalysts. However, it is of great importance in the evaluation of catalyst lifetime. Therefore, we had an attempt to understand of the deactivation of $S_2O_8^{2-}/ZnAl_2O_4$-4 wt%Ce solid acid during the reaction, with the aim to provide the reference data for the further study of SO_4^{2-}/M_xO_y solid acid catalyst. There are only few studies on concerning $S_2O_8^{2-}/ZnAl_2O_4$-*x* wt%Ce solid acid catalysts, which are expected to act as a promising catalyst system and have certain application prospect in the acid catalytic reaction.

2. Experimental

2.1 Catalysts preparation

Solid acid catalysts $S_2O_8^{2-}/ZnAl_2O_4$-*x* wt% Ce (*x*=0, 2, 4, 6, 8, 10) were prepared as follows: 15.004 g $Al(NO_3)_3{\cdot}9H_2O$, 5.950 g $Zn(NO_3)_2{\cdot}6H_2O$ and stoichiometry amounts of $Ce(NO)_3{\cdot}9H_2O$ were dissolved in absolute ethyl alcohol, followed by adding 5 wt% (~1.048 g) of polyethylene glycol to the ethyl alcohol solution with magnetic stirring at room temperature for 4 h. The obtained mixture was evaporated with further stirring for 2 h in a water bath at 60 °C to get the sol. The sol was dried and was grounded into a fine powder. Then, the powder was calcined at 600 °C for 5 h in air sequentially to obtain the spinel $ZnAl_2O_4$-*x* wt%Ce. The $ZnAl_2O_4$-*x* wt%Ce precursors were then sulfated for 12 h by impregnating with 1.50 mol/L $(NH_4)_2S_2O_8$ solution on the proportion of 10 mL/g solution to 1 g precursors. Finally, after having been filtered and dried, the samples were calcined at 550 ℃ for 5 h in air, which subsequently obtain the $S_2O_8^{2-}/ZnAl_2O_4$-*x* wt%Ce catalysts.

2.2 Catalysts characterization

The solid phases of the calcined catalysts were determined by using the X-ray powder diffraction (XRD) (Bruker AXS D8-Focus X diffractometer), using CuKα radiation at 40 kV and 40 mA ; IR spectrum of the catalysts was recorded by a Nicolet 6700 IR spectrometer using the KBr pellet technique; Thermogravimetric analysis (TG) was performed on a STA-409PC thermoanalyzer in the temperature range of 30-1000 ℃ with a heating rate of 20 ℃/min; Scanning Electron Microscopy (SEM) was performed on a SU 8010N electron microscope with an acceleration voltage of 10 Kv; The X-ray photoelectron spectroscopy (XPS) was performed in a VG Multilab 2000; The NH_3 temperature programmed desorption (NH_3-TPD) experiments were carried out using a Micromeritics AutoChem II 2920 quipped with a TCD detector; N_2 adsorption analysis was carried out using micromeritics (ASAP-2020) at liquid nitrogen temperature (77 K), and the surface area was calculated by the BET method and the pore size distribution was obtained from the adsorption isotherm by the BJH method.

2.3 Catalytic activity test

The catalytic activities of the catalysts were tested in a three-necked flask equipped with a magnetic stirrer, a thermometer and a refluxing condenser tube under atmospheric pressure. The reaction conditions were as follows: the range of reaction temperatures was 115-118 ℃, the molar ratio of acetic acid to *n*-butanol was 1:1-1:5; the reaction time was 1.0-4.0 h; the catalyst amount was 0-2.21% (percentage content of the reaction mixture). The initial and residual acid was determined by means of titration. The esterification efficiency of acetic acid can be calculated using the following equation (by the method of GB1668-81):

Esterification efficiency of acetic acid (%) =

$$\frac{M_0 - M_1}{M_0} \times 100$$

Where M_0 is the acid value before reaction and M_1 is the acid value after reaction. 0.50 mL initial or final reaction mixture was added in 20.00 mL absolute alcohol and titrated by 0.10 mol/L NaOH solution using phenolphthalein as an indicator.

In order to test the catalyst lifetime, $S_2O_8^{2-}/ZnAl_2O_4$-4 wt% Ce were repeatedly used for the batch reaction process under the optimum synthesis conditions. After each catalytic evaluation was finished, the catalyst was recovered by filtering and drying and reused for the next evaluation.

3. Results and discussion

3.1 Catalytic activities

Table. 1 showed the effect of *x* value on the catalytic activity of $S_2O_8^{2-}/ZnAl_2O_4$-*x* wt%Ce in esterification of acetic acid with *n*-butanol. For comparison, the catalytic activities of the support of $ZnAl_2O_4$ and $ZnAl_2O_4$-4wt%Ce were also provided in Table 1. It was found that both $ZnAl_2O_4$ and $ZnAl_2O_4$-4wt%Ce showed lower catalytic activity with less than 50% esterification efficiency. However, $S_2O_8^{2-}/ZnAl_2O_4$-*x* wt%Ce catalysts all exhibited significantly high catalytic activities with above 90% esterification efficiency. According to the IR results, their higher catalytic activities of $S_2O_8^{2-}/ZnAl_2O_4$-*x* wt%Ce catalysts were attributed to the formation of the acid structures between sulfuric groups and metal ions. By comparison of $S_2O_8^{2-}/ZnAl_2O_4$, $S_2O_8^{2-}/ZnAl_2O_4$-*x* wt%Ce (*x* = 2-10) catalysts presented better catalytic activities. This result may be caused by the following reasons. First, the cerium addition changed the chemical state of the exterior atom in the spinel lattice of the samples, which was confirmed by the results of XRD and XPS. Correspondingly, the polarization degree of surface elements was increased. As a result, the addition of Ce enhanced the acid strength of $S_2O_8^{2-}/ZnAl_2O_4$-*x* wt%Ce, which was further proved by NH_3-TPD and TG techniques. Secondly, the addition of cerium could strengthen the interaction between $S_2O_8^{2-}$ and metallic ions, which is beneficial to preserve sulfate ions on the surface of catalysts and prevent the loss of $S_2O_8^{2-}$.[20, 23, 24] This was coincident with the experimental results of the reusability, IR and XPS studies. Based on the above analysis, we could assume

that the addition of cerium played an important role in the improvement of acidic property and the catalytic activities of the samples. The similar results were also reported by other literatures. For example, Xiao et al prepared cerium-doped mesoporous TiO_2 nanofiber ($SO_4^{2-}/Ce_x/TiO_2$) solid acid catalysts, and discovered that doping Ce into TiO_2 resulted in the increase of total acidity.[16] Yet, it was worth noting that excess cerium as an assistant component might reduce the number of $S_2O_8^{2-}$ bonding to the surface of metal ions, thereby the acid strength and catalytic activities of the catalysts would drop accordingly. As shown in Table. 1, the appropriate addition of Ce was 4 wt% and $S_2O_8^{2-}/ZnAl_2O_4$-4 wt%Ce exhibited the highest catalytic activity with maximum 95.9% esterification efficiency. Based on the results of NH_3-TPD, this result might be owing to its strongest acid strength and its maximum amount of acid sites in all samples.

Table 1 Effects of *x*-value on the catalytic activities of $S_2O_8^{2-}/ZnAl_2O_4$-*x* wt%Ce in the esterification reaction of acetic acid with *n*-butanol

Catalysts	*x* value	Esterification efficiency (%)
$S_2O_8^{2-}/ZnAl_2O_4$-*x* wt%Ce	0	91.4
	2	94.3
	4	95.9
	6	95.4
	8	94.8
	10	94.8
$ZnAl_2O_4$-*x* wt%Ce	0	45.2
$ZnAl_2O_4$-*x* wt%Ce	4	44.5

The range of reaction temperature was 115~118 ℃; The molar ratio of acetic acid to *n*-butanol was 1:3; the amount of catalyst was 1.55 %; the reaction time was 3 h;

It is well known that the catalyst amounts are closely related with the number of acid center on the surface of the solid acid catalysts, which play an important role in the catalytic activity of the catalysts. Thus, the reaction was studied with different catalyst amounts of $S_2O_8^{2-}/ZnAl_2O_4$-4 wt%Ce. As shown in Table 2, the esterification efficiency was less than 40% when the reaction was carried out without catalyst. The esterification efficiency was obviously improved with the addition of the catalyst. In the meantime, the esterification efficiency was increased with catalyst amounts increasing from 0.37 to 1.55%, which might be attributed to the increase of the number active sites with increasing catalyst amounts. However, the excess acid amount might promote the occurrence of the reverse reaction.[25] Accordingly, the esterification efficiency was reduced slightly when the catalyst amount exceeded 1.55%. Thus, the optimum catalyst amount was considered to be 1.55% with the maximum 95.9% esterification efficiency.

Table 2 gave the effects of the molar ratio of acetic acid to *n*-butanol on the esterification efficiency of $S_2O_8^{2-}/ZnAl_2O_4$-4 wt%Ce. The esterification efficiency was increased obviously with increasing the molar ratio of acetic acid to *n*-butanol from 1:1 to 1:3. This result might be that excess *n*-butanol was usually beneficial to push the reversible reaction forward, which resulted in the increase of the esterification efficiency. However, a mass of *n*-butanol might dilute the concentration of the acid, so there was no obvious change in the esterification efficiency when the molar ratio of acetic acid to *n*-butanol was beyond 1:3.[26] Thereby, the molar ratio of 1:3 was sufficient to achieve a high catalytic activity.

The reaction time is one of the most important factors that affect the catalytic activity of the catalysts. The effects of the reaction time on the catalytic activity of $S_2O_8^{2-}/ZnAl_2O_4$-4 wt%Ce were examined. As listed in Table 2, the longer reaction time would lead to the esterification rate increase rapidly when the reaction time was less than 3 h. And then, the esterification efficiency had leveled off at around 96% in longer duration of reaction. So, 3 h was sufficient for the completion of the esterification reaction.

Table 2 The effect of reaction conditions on catalytic activities of $S_2O_8^{2-}/ZnAl_2O_4$-4 wt%Ce

Catalyst	Amount [a]	Time (h)	a : *n* [b] ratio	Esterification efficiency (%)
$S_2O_8^{2-}/ZnAl_2O_4$-4 wt%Ce	1.55	3.0	1:1	57.1
	1.55	3.0	1:2	86.2
	1.55	3.0	1:3	95.9
	1.55	3.0	1:4	95.9
	1.55	3.0	1:5	95.9
	0.00	3.0	1:3	38.0
	0.37	3.0	1:3	79.6
	0.73	3.0	1:3	83.4
	1.14	3.0	1:3	88.7
	1.85	3.0	1:3	95.8
	2.21	3.0	1:3	95.1
	1.55	1.5	1:3	86.6
	1.55	2.0	1:3	91.8
	1.55	2.5	1:3	94.4
	1.55	3.5	1:3	96.5
	1.55	4.0	1:3	96.8

[a] the amount was calculated on the basis of total weight of the reactants

[b] the molar ratio of acetic acid to *n*-butanol

It is well known that SO_4^{2-}/M_xO_y solid acid catalysts commonly suffer from rapid deactivation and low service life despite of their high initial activities, which is mainly owing to the loss of sulfur species as well as carbon deposition. [9] For example, Shi had reported that the catalytic activities of sulfate-promoted iron oxide dropped from 84.48 % to 51.48 % after 10 recycles in the *n*-butyl acetate esterification.[27] In fact, deactivation is a general problem and a rather complicated phenomenon in heterogeneous catalysis, which is also the main problem faced by SO_4^{2-}/M_xO_y solid acid catalysts. [2] Thus, the reusability and its improvement are of great importance in the study of SO_4^{2-}/M_xO_y solid acid catalysts. In view of this point, $S_2O_8^{2-}/ZnAl_2O_4$ and $S_2O_8^{2-}/ZnAl_2O_4$-4 wt%Ce solid acid catalysts were recycled to study the stability of the catalysts under the same synthesis conditions. The results were presented in Fig. 1. It could be seen clearly that the addition of Ce played a very important role in improving the lifetime and the stability of the catalyst. Compared with $S_2O_8^{2-}/ZnAl_2O_4$, $S_2O_8^{2-}/ZnAl_2O_4$-4 wt%Ce solid acid catalyst showed the obviously better reusability, which remained above 80% esterification even after being used for six times. This result might be attribute to its excellent structural stability and excellent resistance to the loss of the sulfur species. This result was also in agreement with other literature.[28]

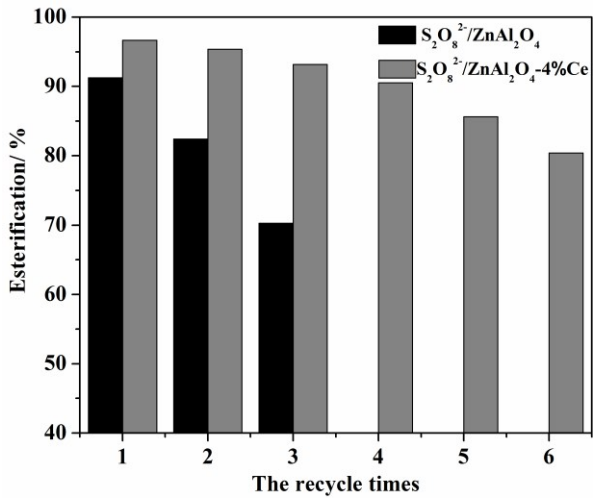

Fig.1 Reusability of $S_2O_8^{2-}/ZnAl_2O_4$ and $S_2O_8^{2-}/ZnAl_2O_4$-4 wt%Ce in the esterification reaction of acetic acid with n-butanol.(The range of reaction temperature was 115~118 °C; the molar ratio of acetic acid to *n*-butanol was 1:3; the reaction time was 3 h, the amount of catalysts was 1.55 %.)

Table 3 demonstrated the comparison of $S_2O_8^{2-}/ZnAl_2O_4$-4 wt%Ce with other reported solid acid catalysts. The catalytic activity of $S_2O_8^{2-}/ZnAl_2O_4$-4 wt%Ce is comparable with the series of SO_4^{2-}–$Ce_{0.02}/TiO_2$,[16] mesoporous materials catalyst,[29] and other type solid acid catalysts[30-32] in this esterification reaction. However, crystal structure transformation was generally occurred in the synthesis and modification of SO_4^{2-}/TiO_2, which directly influenced their catalytic activities.[12, 13] In this present work, composite oxide spinel $ZnAl_2O_4$ as a new superior system for synthesis of $S_2O_8^{2-}/ZnAl_2O_4$-*x* wt%Ce solid acid catalysts exhibited the characteristic advantages of the simple crystal structure and excellent structure stability in the process of synthesis and modification. Besides, $S_2O_8^{2-}/ZnAl_2O_4$-*x* wt%Ce solid acid catalysts had the advantages of easier preparation and lower cost compared to other type solid acid catalysts as shown in Table 3.

Table 3 Comparison of $S_2O_8^{2-}/ZnAl_2O_4$-4 wt%Ce catalysts with other reported solid acid catalysts

Catalyst	Reaction conditions			Esterification efficiency (%)	Refs.
	a : *n*[a] ratio	amount[b] (wt%)	Reaction time (h)		
$S_2O_8^{2-}/ZnAl_2O_4$-4 wt%Ce	1:3	1.55	3	95.9	Present work
SO_4^{2-}–TiO_2	1:3	2	0.75	60.1	[16]
SO_4^{2-}–$Ce_{0.02}/TiO_2$	1:3	2	0.75	97.1	[16]
Mesoporous resin -SO_3H	1.5:1	0.12	4	97.6	[29]
Mesoporous carbon -SO_3H	1.5:1	0.12	4	96.8	[29]
$[TPSPP]_3PW_{12}O_{40}$	1:1.2	5.38	1.5	97	[30]
20% TPA /AT-GMB	3:1	2.36	12	88	[31]
sulfate-promoted iron oxide	1:1.56	4.88	1	84.5	[27]
10 wt% MoO_3/Al_2O_3	1:3	1	2	81	[32]

[a] The molar ratio of acetic acid to *n*-butanol

[b] Catalyst amount is calculated on the basis of total weight of the reactants

3.2 Catalytic Characterization

In order to understand the crystal transformation process, Fig. 2 showed XRD pattern of $ZnAl_2O_4$- *x* wt%Ce (a) and $S_2O_8^{2-}/ZnAl_2O_4$-*x* wt%Ce solid acid catalyst (b). As shown in Fig. 2 (a), the diffraction peaks at 2θ =18.9 °, 31.4 °, 36.90 °, 44.2 °, 49.2 °, 55.8°◦, 59.5° and 65.4° were observed in $ZnAl_2O_4$-*x* wt%Ce, which were the characteristic of $ZnAl_2O_4$ spinel phase (PDF No. 73-1961). Similar peaks were also observed in $S_2O_8^{2-}/ZnAl_2O_4$-*x* wt%Ce solid acid catalysts (shown in Fig. 2 (b)), indicating that the carrier spinel of $ZnAl_2O_4$ had the prominent advantages of single crystal shape and stable structure in the process of modification and sulfation. However, there were also some differences in the samples. Compared with $ZnAl_2O_4$, $ZnAl_2O_4$-*x* wt%Ce (*x*= 2, 4, 6, 8, 10) displayed the new diffraction peaks of CeO_2 because of cerium addition. Moreover, the characteristic peaks of CeO_2 became stronger with the increase of Ce doping amount, indicating that Ce mainly existed in the form of CeO_2. Besides, the weak diffraction peaks of ZnO phase were also observed in all samples of $ZnAl_2O_4$-*x* wt%Ce (*x*=2, 4, 6, 8, 10), which might be related to the change of the chemical environment in the spinel lattice because of the cerium addition. $ZnSO_4 \cdot H_2O$ and $Al_2(SO_4)_3$ crystalline phases were observed in all samples of $S_2O_8^{2-}/ZnAl_2O_4$-*x* wt%Ce by comparison with $ZnAl_2O_4$- *x* wt%Ce. It might be attributed to the interaction between excess $S_2O_8^{2-}$ and metal ions.[33, 34] A similar phenomenon was also observed in other SO_4^{2-}/M_xO_y solid acid catalysts.[35, 36] In addition, the characteristics diffraction peaks of CeO_2 became unapparent in all samples of $S_2O_8^{2-}/ZnAl_2O_4$-*x* wt%Ce, which might be of high dispersions or amorphous phases. In the meantime, the characteristics diffraction peaks of ZnO were not detected in all samples of $S_2O_8^{2-}/ZnAl_2O_4$-*x* wt%Ce, suggesting that Zn^{2+} might be in the form of $ZnSO_4 \cdot H_2O$.

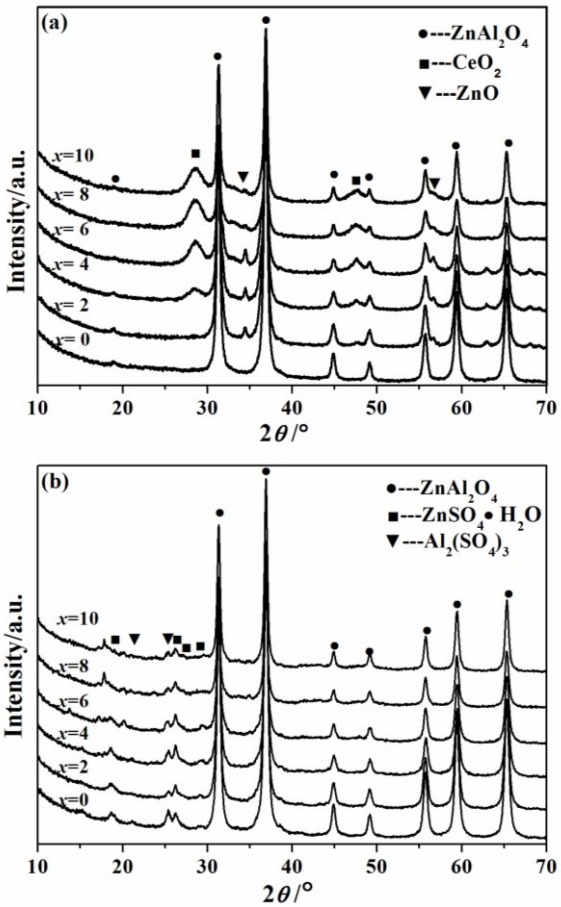

Fig. 2 XRD pattern of $ZnAl_2O_4$-*x* wt%Ce (a) and $S_2O_8^{2-}/ZnAl_2O_4$-*x* wt%Ce solid acid catalyst(b).

Fig. 3 recorded the FT-IR spectra of $S_2O_8^{2-}/ZnAl_2O_4$- *x* wt%Ce solid acid catalysts. Three strong bands around 670 cm^{-1}, 557 cm^{-1} and 497 cm^{-1} were attributed to Al-O stretching vibrations, Zn-O stretching vibrations and Al-O bending vibrations, respectively, which belonged to spinel-type $ZnAl_2O_4$ structure.[37] This result was in good agreement with the XRD results. The special bands in the range of 900-1400 cm^{-1} were detected in all samples and characterized the active acid structures of the catalysts.[38] The specific bands in this region were attributed to the strong interaction between sulfuric groups and metal ions, which were correlated to their high catalytic activities. Among them, the bands at 975 cm^{-1}, 1110 cm^{-1} and 1180 cm^{-1} corresponded to the symmetric and asymmetric stretching vibration of S-O bonds, respectively.[39] The band at 1398 cm^{-1} was attributed to the symmetric and asymmetric stretching mode of S=O, respectively.[40] The suction-induced complex S=O improved the electron-accepting capability of the metal atoms, which made the samples possess super acid sites.[41] Besides, the band located at 1635 cm^{-1} was assigned to the deformation vibration of the adsorbed water.[42] In order to evaluate the structural stability, Fig. 3 also showed the IR spectra of $S_2O_8^{2-}/ZnAl_2O_4$-4 wt%Ce after being used repeatedly for six times. By contrast with the fresh catalyst, the typical bands at 670 cm^{-1}, 557 cm^{-1} and 497 cm^{-1} were still observed in $S_2O_8^{2-}/ZnAl_2O_4$-4 wt%Ce after being used repeatedly for six times, indicating that it had excellent structural stability. In particular, $S_2O_8^{2-}/ZnAl_2O_4$-4 wt%Ce showed similar intensity and characteristics bands in the range of 1400-900 cm^{-1} after being used repeatedly for six times. This result suggested that $S_2O_8^{2-}/ZnAl_2O_4$-4 wt%Ce also presented excellent resistance to the loss of the sulfur species, which might be one of the important reasons for its better reusability.

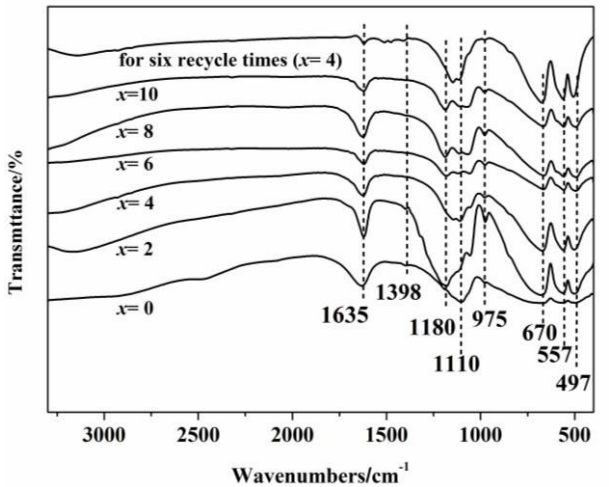

Fig. 3 IR spectra of $S_2O_8^{2-}/ZnAl_2O_4$-*x* wt%Ce before reaction and $S_2O_8^{2-}/ZnAl_2O_4$-4 wt%Ce after being used repeatedly for six times

To probe the element type and element valence state on the surface of the catalysts, XPS analysis for $S_2O_8^{2-}/ZnAl_2O_4$ and $S_2O_8^{2-}/ZnAl_2O_4$-4 wt%Ce was performed. It was found Zn atom maintained the same chemical valence states in two samples.[43] Two peaks corresponding to Zn 2p3/2 and Zn 2p1/2 were all located at 1022.1 eV and 1045.1 eV in the two samples, respectively. However, the addition of Ce had a certain affect on the chemical valence states of Al atom, O atom and S atom. Accordingly, there were some significant differences in the XPS spectra of the two samples. Compared with $S_2O_8^{2-}/ZnAl_2O_4$, there were higher binding energy of Al 2p, O 1s and S 2p in the XPS spectra of $S_2O_8^{2-}/ZnAl_2O_4$-4 wt%Ce. The change of the electron binding energy was resulted from the different chemical environment of the atoms. So, we could suppose that the addition of Ce might affect the interaction between atoms and atom type in combination with each other. From the result of catalytic activity, it was apparently demonstrated that $S_2O_8^{2-}/ZnAl_2O_4$-4 wt%Ce had higher catalytic activity and better reusability than $S_2O_8^{2-}/ZnAl_2O_4$. XPS analysis in this section might be one of the possible explanations for this result. The peaks at 886.1, 897.3 and 904.8 eV were corresponding to Ce 3d binding energy, demonstrating the cerium oxidation state was +4.[44, 45] As shown in Fig. 4, Ce was observed in the XPS spectra of $S_2O_8^{2-}/ZnAl_2O_4$-4 wt%Ce, indicating that Ce had been successfully introduced to the catalyst. With reference to the XRD result, the intensity of CeO_2 diffraction peaks became not apparent in the sample. So, the detection of the Ce in XPS result further evidenced that CeO_2 might be highly dispersed in the sample. In addition, it is noted that the peak corresponding to S 2p binding energy was clearly observed in the two samples, which was assigned to the sulfur oxidation state of +6.[46] It is well known that S^{6+} plays a key role on the formation of the acidity structure. The suction-induced complex S=O promotes the electron-accepting ability for the metal atoms, making the samples possess supper acid. Accordingly, IR spectra of $S_2O_8^{2-}/ZnAl_2O_4$-4 wt%Ce showed the

special bands in the range of 900-1400 cm^{-1}, which were correlated to the active acid structures of the catalysts.

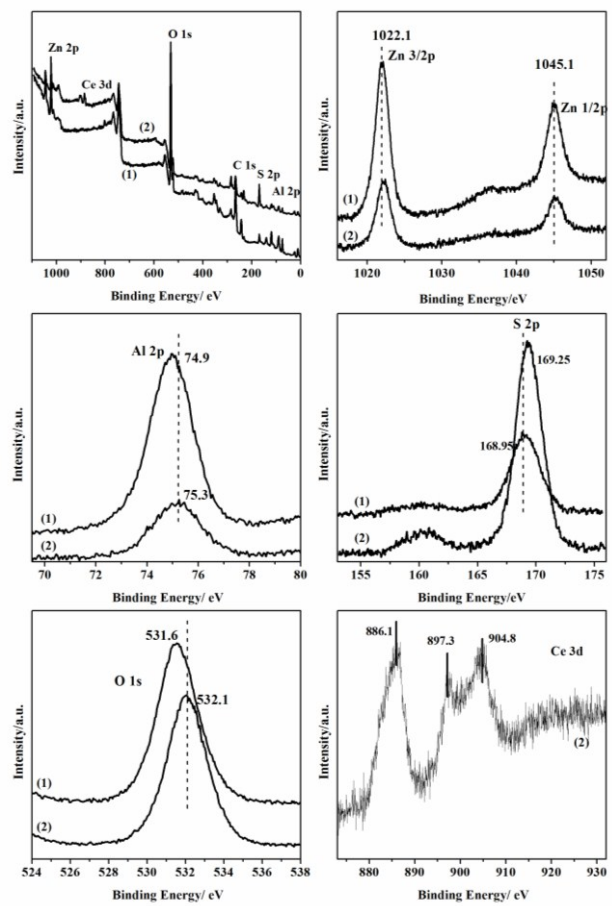

Fig. 4 XPS spectra of $S_2O_8^{2-}/ZnAl_2O_4$ and $S_2O_8^{2-}/ZnAl_2O_4$ -4 wt%Ce.(1) $S_2O_8^{2-}/ZnAl_2O_4$; (2) $S_2O_8^{2-}/ZnAl_2O_4$ -4 wt%Ce

In order to examine the thermostability of the catalysts, the TG analysis was showed in Fig. 5. The TG curve exhibited three weight loss stages of the two samples. The first weight loss below 400℃ belonged to desorption of the physical adsorbed water. The second weight loss between 400 ℃ and 600 ℃ was assigned to the dehydroxylation or the removal of $S_2O_8^{2-}$ from the surface of the catalysts. The third weight loss at a higher temperature range between 600 and 1000 ℃ was due to the gradual decomposition of the sulfur species on the surface of the catalysts.[39] So, the third weight loss above 600℃ was closely related to the sulphur content and the acid sites on the surface of the samples. By contrast, the fresh $S_2O_8^{2-}/ZnAl_2O_4$-4 wt%Ce gave the mass weight loss of 15.89% above 600℃. But, the fresh $S_2O_8^{2-}/ZnAl_2O_4$ had the relatively little weight loss of 8.03% above 600℃. This result revealed that the addition of Ce was beneficial to improve the number of acid center and the acid strength, making the catalytic activity of $S_2O_8^{2-}/ZnAl_2O_4$-4 wt%Ce increase. This result was not only identified by NH_3-TPD analysis, but also was in good consistent with the results of the catalytic activities. For the used catalysts, there was still some weight loss between 600 ℃ and 1000 ℃, making the used catalysts still keep a certain catalytic activity. Comparing the used catalysts with the fresh catalysts, the weight loss between 600 ℃ and 1000 ℃ was significantly reduced. The weight loss of 15.89% in the fresh $S_2O_8^{2-}/ZnAl_2O_4$-4 wt%Ce was changed into the weight loss of 7.98% in the used $S_2O_8^{2-}/ZnAl_2O_4$-4 wt%Ce. For the used $S_2O_8^{2-}/ZnAl_2O_4$, the weight loss between 600 ℃ and 1000 ℃ was also reduced to 2.41%. The above results proved that the loss of sulfur species would inevitably occur in the process of acid catalytic reaction, which was the one of an important reasons to cause catalyst deactivation.[29] This result was in good well with the result of the catalyst stability.

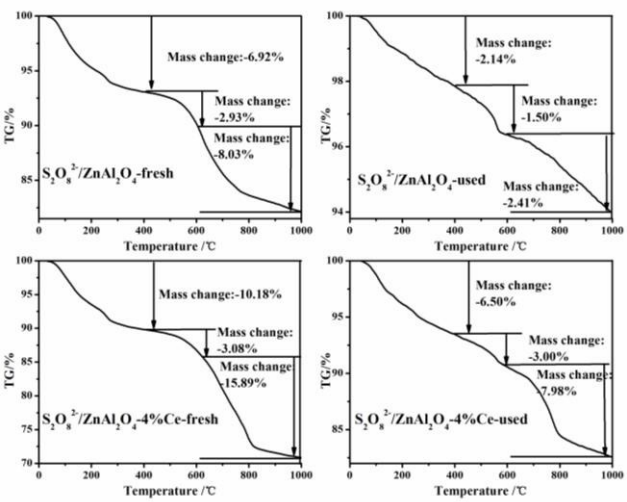

Fig. 5 TG curves of fresh and used $S_2O_8^{2-}/ZnAl_2O_4$-x wt%Ce catalysts (x=0, 4)

The NH_3-TPD results was used to determine the acid strength distribution from the desorption temperature of NH_3. The higher the desorption peak temperatures was, the stronger the acid strength was.[40] Generally, the peaks below 450 ℃ were believed to be caused by the absorption of weak and moderate intensity. The second peaks between 450 ℃ and 650 ℃ were attributed to strong acidic sites. The last peaks above 650 ℃ belonged to super strong acidic sites.[47] As shown in Fig. 6 (a), all the samples showed the prominent broad desorption peaks in the range of 100 ℃ to 700 ℃. Among them, the TPD profiles of $S_2O_8^{2-}/ZnAl_2O_4$ revealed two peaks of NH_3 desorption, one was in the range of 100 ℃ to 450 ℃ and another one was between 450 ℃ and 650 ℃, suggesting the presence of weak, moderate and strong acidic sites. Assuming that the peak area was proportional to the amount of the acid site, the intensity of weak and moderate acid sites was evident higher than that of strong acid sites in the case of $S_2O_8^{2-}/ZnAl_2O_4$ solid acid catalyst. The TPD profiles of $S_2O_8^{2-}/ZnAl_2O_4$-2 wt%Ce and $S_2O_8^{2-}/ZnAl_2O_4$-6 wt%Ce catalysts gave broad ammonia desorption peaks in the range of 450 ℃ and 650 ℃ with certain intensity, indicating the high concentration of strong acidic sites. The TPD profiles of $S_2O_8^{2-}/ZnAl_2O_4$-4 wt%Ce catalyst exhibited three distinct peaks of NH_3 desorption, two were between 450 ℃ and 650 ℃ and another one was at above 650 ℃. Specifically, the NH_3 desorption peak above 650 ℃ was observed with high intensity, suggesting the high concentration of super acidic sites.[48] Compared with $S_2O_8^{2-}/ZnAl_2O_4$, $S_2O_8^{2-}/ZnAl_2O_4$-*x* wt%Ce had the stronger acid strength. This result further demonstrated that the addition of Ce contributed to improve the number of acid center and the acid strength, which was consistent well with the results of the XPS and TG analysis.

This could be the main reason for the higher catalytic activity of $S_2O_8^{2-}/ZnAl_2O_4$-*x* wt%Ce. Based on NH_3-TPD results, it was clearly observed that the $S_2O_8^{2-}/ZnAl_2O_4$-4 wt%Ce catalyst exhibited the highest acid strength and had the maximum number of acidic sites.

It is worthwhile to investigate the reasons for the deactivation of SO_4^{2-}/M_xO_y solid acid catalysts. The above TG analysis speculated that the loss of sulfur species on the surface of $S_2O_8^{2-}/ZnAl_2O_4$-4 wt%Ce solid acid may be one of the reasons for its deactivation during the acid catalyzed reaction. In order to further explore the reason for the deactivation in the process of the reaction, Fig. 6 (b) gave the TPD profiles of three samples, including fresh $S_2O_8^{2-}/ZnAl_2O_4$-4 wt%Ce, $S_2O_8^{2-}/ZnAl_2O_4$-4 wt%Ce after being used repeatedly for the first time and six times. It was observed that the intensity of the peak above 650 ℃ become weaker with increasing the catalyst reuse times. Furthermore, it was also found that the amount of the acidic sites became less and less with the increase of the catalyst reuse times. After the catalyst being used repeatedly for six times, the peak above 650 ℃ was not detected and the amount of the acidic sites was decreased. Correspondingly, the catalytic activity was reduced. Combining the results of NH_3-TPD with TG analysis, it might be concluded that $S_2O_8^{2-}/ZnAl_2O_4$-4 wt%Ce solid acid inevitable suffered from the loss of sulfur species, reducing the acid strength and decreasing the amount of the acidic sites. This was one of the essential reasons for the deactivation of $S_2O_8^{2-}/ZnAl_2O_4$-4 wt%Ce solid acid during the reaction. The result also had certain reference value for other SO_4^{2-}/M_xO_y solid acid catalysts.

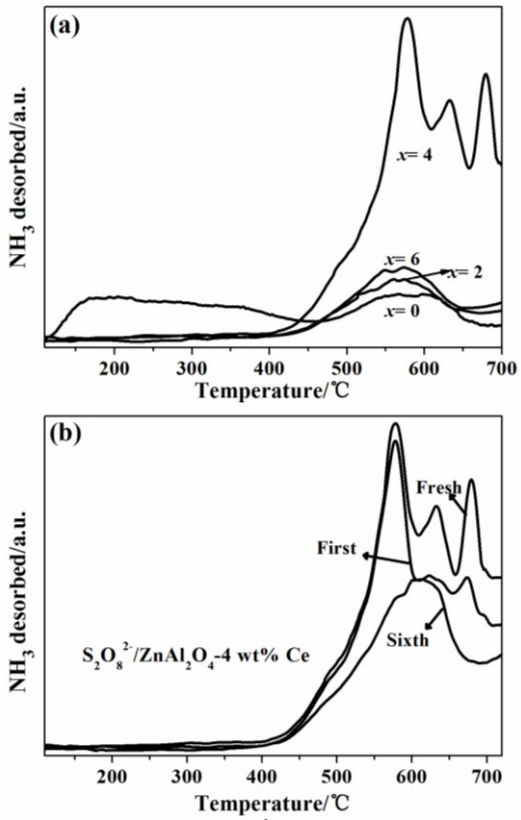

Fig. 6 NH_3-TPD spectra of fresh $S_2O_8^{2-}/ZnAl_2O_4$-*x* wt%Ce (x=0, 2, 4, 6) (a) and used $S_2O_8^{2-}/ZnAl_2O_4$-4 wt%Ce (b)

SEM images of fresh $S_2O_8^{2-}/ZnAl_2O_4$-4 wt%Ce and $S_2O_8^{2-}/ZnAl_2O_4$-4 wt%Ce after being used repeatedly for six times were shown in Fig. 7. The fresh $S_2O_8^{2-}/ZnAl_2O_4$-4 wt%Ce displayed an aggregated-nanosheet appearance on the surface, which might be beneficial to the increase of the acid sites and the improvement of the catalytic activity. [49] The catalyst after being used repeatedly for six times had slightly particles agglomeration. Combining with the experimental results of N_2 adsorption analysis (as shown in Fig. 8), the N_2 adsorption-desorption isotherms of both fresh and used catalysts showed the typical IV isotherm with the hysteresis loop in the low relative (P/P_0) range of 0.4−1, indicating their representative mesoporous structures. Besides, the average pore size of fresh and used catalysts was 9.5 nm and 10.7 nm, respectively. In addition, Fig. 8 showed that the BET surface area of fresh $S_2O_8^{2-}/ZnAl_2O_4$-4 wt%Ce was 21.1 m^2/g. Whereas, $S_2O_8^{2-}/ZnAl_2O_4$-4 wt%Ce after being used repeatedly for six times was reduced to the 11.0 m^2/g, which was probably due to the particles agglomeration as demonstrated by SEM images. The particles agglomeration and the decrease of the specific surface area might be the reasons for its decrease in the catalytic activity of $S_2O_8^{2-}/ZnAl_2O_4$-4 wt%Ce after being used repeatedly for six times.

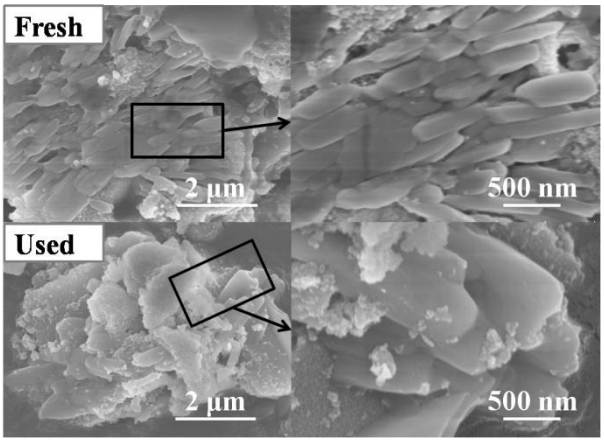

Fig. 7 SEM images of fresh $S_2O_8^{2-}/ZnAl_2O_4$-4 wt%Ce and $S_2O_8^{2-}/ZnAl_2O_4$-4 wt%Ce after being used repeatedly for six times

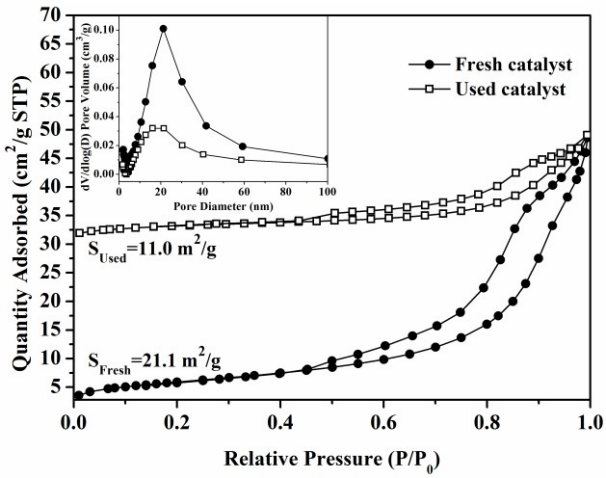

Fig. 8 N_2 adsorption-desorption isotherms and pore-size distributions of fresh $S_2O_8^{2-}/ZnAl_2O_4$-4 wt%Ce and $S_2O_8^{2-}/ZnAl_2O_4$-4 wt%Ce after being

used repeatedly for six times

Conclusions

A new series of $S_2O_8^{2-}/ZnAl_2O_4$-*x* wt%Ce solid acid catalyst with stable spinel structures were successfully prepared by modifying $S_2O_8^{2-}/ZnAl_2O_4$ with Ce. The improved catalysis performance of Ce-modified $S_2O_8^{2-}/ZnAl_2O_4$ was attributed to the reasons that the addition of Ce improved the stability of the sulfur species and the acid strength of $S_2O_8^{2-}/ZnAl_2O_4$-*x* wt%Ce. Among them, the $S_2O_8^{2-}/ZnAl_2O_4$-4 wt%Ce catalyst performed the highest catalytic activity, which was ascribe to its highest acid strength and the maximum number of acidic sites. In addition, the optimum synthesis conditions over $S_2O_8^{2-}/ZnAl_2O_4$-4 wt%Ce solid acid catalyst were as follows: the molar ratio of acetic acid to *n*-butanol was 1:3; catalyst amount was 1.55%; reaction time was 3 h. Under the optimum synthesis conditions, the esterification efficiency over $S_2O_8^{2-}/ZnAl_2O_4$-4 wt%Ce was up to 95.9%. Compared with unmodified $S_2O_8^{2-}/ZnAl_2O_4$, $S_2O_8^{2-}/ZnAl_2O_4$-4 wt%Ce solid acid catalyst showed the obviously better reusability, which might be attribute to its excellent structural stability and excellent resistance to the loss of the sulfur species. However, the loss of sulfur species would still inevitably occur in the process of acid catalytic reaction, which was one of an important reason to cause catalyst deactivation. At present, $S_2O_8^{2-}/ZnAl_2O_4$-*x* wt%Ce solid acid catalysts have not yet been extensively studied. The obtained results provided the possibility to prepare a large variety of solid acids based on composite oxide spinel.

Acknowledgments

The authors gratefully acknowledge the financial support from NSFC (21203170 and 41172051), ERCNGME (CUGNGM 20133), Self-DIRFC (2013-09) and NCSITP (201310491019 and 201510491034).

Notes and references

[a] *Faculty of Materials Science and Chemistry, Engineering Research Center of Nano-Geomaterials of Ministry of Education, China University of Geosciences, Wuhan 430074, China. E-mail address: wjx76@sina.com Tel/ fax: +86-27-87407079*

1 P. Barbaro, L. Gonsalvi, A. Guerriero and F. Liguori, Green Chem., 2012, **14**, 3211-3219.
2 J. M. Fraile, E. García-Bordejé and L. Roldán, J. Catal., 2012, **289**, 73-79.
3 W.K. Yao, J. Li, Y. Feng, W. Wang, X.L. Zhang, Q. Chen, S. Komarneni and Y.J. Wang, RSC Adv., 2015, **5**, 30485-30494.
4 A. Corma, A. Martínez and C. Martínez, J. Catal. 1996, **164**, 422-432.
5 E.L.S. Ngee, Y.J. Gao, X. Chen, T.M. Lee, Z.G. Hu, D. Zhao and N. Yan, Ind. Eng. Chem. Res., 2014, **53**, 14225-14233.
6 S. Blagov, S. Parada, O. Bailer, P. Moritz, D. Lam, R. Weinand and H. Hasse, Chem. Engi. Sci., 2006, **61**, 753-76.
7 F.C. Zheng, Q.W. Chen, L. Hu, N. Yan and X.K. Kong, Dalton Trans., 2014, **43**, 1220-1227.
8 Y.W. Peng, Z.G. Hu, Y.J. Gao, D.Q. Yuan, Z.X. Kang, Y.H. Qian, N. Yan and D. Zhao, Chem. Sus. Chem., 2015, **8**, 3208-3212.
9 X.J. Shi, Y.L. Wu, P.P. Li, H.F. Yi, M.D. Yang and G.H. Wang, Carbohydr. Res., 2011, **346**, 480-487.
10 F. Su and Y.H. Guo, Green Chem., 2014, **16**, 2934-2957.
11 A. Osatiashtiani, A.F. Lee, D.R. Brown, J.A. Melero, G. Moralese and K. Wilson, Catal. Sci. Technol., 2014, **4**, 333-342.
12 D.E. López, J.G. Goodwin, D.A. Bruce and E. Lotero, Appl. Catal. A: Gen., 2005, **295**, 97-105.
13 M.E. Sad, C.L. Padró and C.R. Apesteguía, Appl. Catal. A: Gen., 2014, **475**, 305-313.
14 K. Takao, Catal. Today, 2003, **81**, 57-63.
15 K. Joseph Antony Raj, M.G. Prakash and B. Viswanathan, Catal. Sci. Technol., 2011, **1**, 1182-1188.
16 G. Xiao, J.F. Zhou, X. Huang, X.P. Liao and B. Shi, RSC Adv., 2014, **4,** 4010-4019.
17 J.R. Sohn and D.C. Shin, Appl. Catal. B, 2008, **77**, 386-394.
18 J.Y. Song, S.H. Chung, M.S. Kim, M.G. Seo, Y.H. Lee, K.Y. Lee and J.S. Kim, J. Mol. Catal. A: Chem., 2013, **370**, 50-55.
19 L. Li, S.W. Liu, J.M. Xu, S.T. Yu, F.S. Liu, C.X. Xie, X.P. Ge and J.Y. Ren, J. Mol. Catal. A: Chem., 2013, **368-369**, 24-30.
20 G.D. Yadav and R.V. Sharma, J. Catal., 2014, **311**, 121-128.
21 D.H. Guan, M.Q. Fan, J. Wang, Y. Zhang, Q. Liu and X.Y. Jing, Mater. Chem. Phys., 2010, **122**, 278-283.
22 A.Q. Wang, X.L. Wu, J.X. Wang, H. Pan, X.Y. Tian and Y.L. Xing, RSC Adv., 2015, **5**, 19652-19658.
23 G.D. Fan, M. Shen, Z. Zhang and F.R. Jia, J. Rare Earths, 2009, **27**, 437-442.
24 H. Zhao, P.P. Jiang, Y.M. Dong, M. Huang and B.L. Liu, New J. Chem., 2014, **38**, 4541-4548.
25 T.F. Parangi, B.N. Wani and U. V. Chudasama, Ind. Eng. Chem. Res., 2013, **52**, 8969-8977
26 G. Kuriakose and N. Nagaraju, J. Mol. Catal. A: Chem., 2004, **223,** 155-159.
27 W.P. Shi and J.W. Li, Catal. Lett., 2013, **143**, 1285-1293.
28 J. R. Sohn, S. H. Lee and J. S. Lim, Catal. Today, 2006, **116**, 143-150.
29 F.J. Liu, J. Sun, Q. Sun, L.F. Zhu, L. Wang, X.J. Meng, C.Z. Qi and F.S. Xiao, Catal. Today, 2012, **186**, 115-120.
30 W.H. Zhang, Y. Leng, D.R. Zhu, Y.J. Wu and J. Wang, Catal. Commun., 2009, **11**, 151-154.
31 S.K. Bhorodwaj and D.K. Dutta, Appl. Clay Sci., 2011, **53**, 347–352.
32 G. Mitran, É. MakÓ, Á. Rédey and I.C. Marcu, Catal. Lett., 2010, **140**, 32-37.
33 K.H. Jiang, D.M. Tong, J.Q. Tang, R.L. Song and C.W. Hu, Appl. Catal. A: Gen., 2010, **389**, 46-51.
34 R.P. Yao, M.J. Zhang, J. Yang, D.L. Yi, J. Xu, F. Deng, Y. Yue and C.H. Ye, Aata Chim. Sinica, 2005, **63**, 269-273.
35 H.P. Yan, Y. Yang, D.M. Tong, X. Xiang and C.W. Hu, Catal. Commun., 2009, **10**, 1558-1563.
36 J.C. Martín, S.B. Rasmussen, S. Suárez, M. Yates, F.J. Gil-Llambías, M. Villarroel and P. Ávila, Appl. Catal. B, 2009, **91**, 423-427.
37 S. Farhadi and S. Panahandehjoo, Appl. Catal. A: Gen., 2010, **382**, 293-302.
38 G.D. Yadav and B.A. Gawade, Catal. Today, 2013, **207**, 145-152.
39 W.P. Shi, Catal. Lett., 2013, **143**, 732-738.
40 P.F. Chen, M.X. Du, H. Lei, Y. Wang, G.L. Zhang, F.B. Zhang and X.B. Fan, Catal. Commun., 2012, **18**, 47-50.
41 L.J. Liu, G.L. Zhang, L. Wang, T. Huang and L. Qin, Ind. Eng. Chem. Res., 2011, **50**, 7219-7227.
42 Y.J. Wu, L. Qin, G. L. Zhang, L. Chen, X. W. Guo and M. Liu, Ind. Eng. Chem. Res., 2013, **52**, 16698-16708.
43 L. Zhang, J.H. Yan, M.J. Zhou, Y.H. Yang and Y. N. Liu, Appl. Surf. Sci., 2013, **268**, 237- 245.
44 S. Lou, T.D. Nguyen-Phan, A.C. Johnston-Peck, L. Barrio, S. Sallis, D.A. Arena, S. Kundu, W.Q. Xu, L.F.J. Piper, E.A. Stach, D.E. Polyansky, E. Fujita, J.A. Rodriguez and S.D. Senanayake, J. Phys. Chem. C, 2015, **119**, 2669 -2679.
45 P. Sudarsanam, B. Mallesham, P.S. Reddy, D. Großmann, W. Grünert and B.M. Reddy, Appl. Catal. B, 2014, **144**, 900-908.
46 C.W. Dunnill, Z.A. Aiken, A. Kafizas, J. Pratten, M. Wilson, D.J. Morgan and I.P. Parkin, J. Mater. Chem., 2009, **19**, 8747-8754.
47 H. Pan, J.X. Wang, L. Chen, G.H. Su, J.M. Cui, D.W. Meng and X.L. Wu, Catal. Commun., 2013, **35**, 27-31.
48 C.C. Hwang and C.Y. Mou, Appl. Catal. A: Gen., 2009, **365**, 173-179.
49 C. Tagusagawa, A. Takagaki, K. Takanabe, K. Ebitani, S. Hayashi and K. Domen, J. Catal., 2010, **270**, 206-212

Synthesis, characterization and properties of Ce-modified $S_2O_8^{2-}/ZnAl_2O_4$ solid acid catalysts

Jun-Xia Wang,* An-Qi Wang, Yu-Lin Xing, Zheng-Xin Zhu, Xiu-Ling Wu, Yong-Qian Wang and Li-Xia Yang

Faculty of Materials Science and Chemistry, Engineering Research Center of Nano-Geomaterials of Ministry of Education, China University of Geosciences, Wuhan 430074, China.

*Corresponding author: Junxia Wang. Tel/ fax: +86 27 87407079; E-mail address: wjx76@sina.com (J. X. Wang)

Graphical abstract

A new spinel solid acid catalyst of $S_2O_8^{2-}/ZnAl_2O_4$-*x* wt%Ce was simply prepared by modifying $S_2O_8^{2-}/ZnAl_2O_4$ with Ce for acid catalysis of acetic acid and *n*-butanol. The addition of Ce played a key role in stabilizing the surface sulfur species and consequently increasing the acid strength of $S_2O_8^{2-}/ZnAl_2O_4$-*x* wt%Ce. The appropriate modification of Ce was 4 wt% and $S_2O_8^{2-}/ZnAl_2O_4$-4 wt%Ce catalyst had 95.86% esterification efficiency under the optimum reaction conditions. Compared with unmodified $S_2O_8^{2-}/ZnAl_2O_4$ catalyst, $S_2O_8^{2-}/ZnAl_2O_4$-4 wt%Ce solid acid catalyst showed much better reusability, which could remain above 80% esterification even after being used for six times.

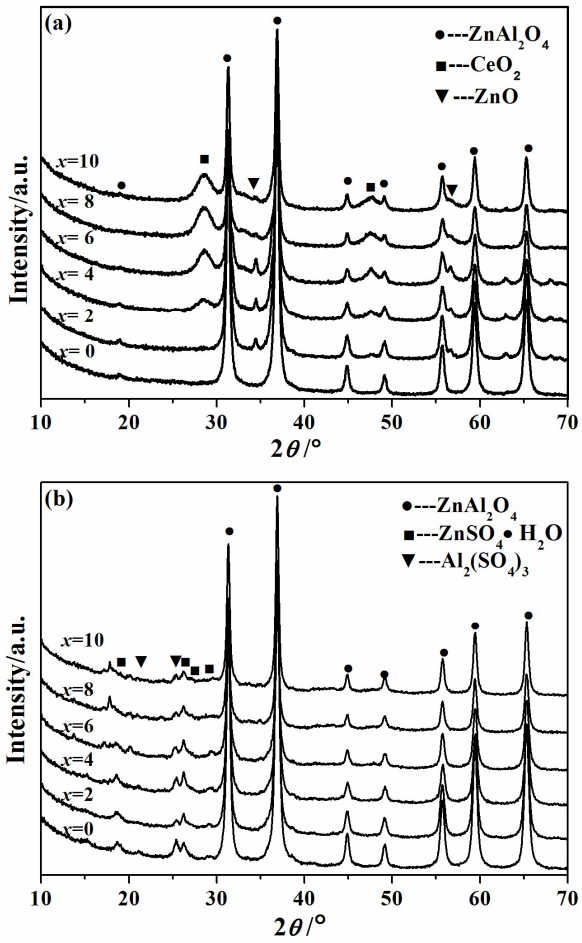

XRD pattern of $ZnAl_2O_4$-*x* wt%Ce (a) and $S_2O_8^{2-}/ZnAl_2O_4$-*x* wt%Ce solid acid catalyst (b)